Spectral shape of Mössbauer absorption for grade-structured systems of interacting particles

M. Hayashi
Physics Department, Toyama Medical and Pharmaceutical University, Toyama, 930-01, Japan
(Received 26 May 1992; revised manuscript received 22 March 1993)

Exact formulas for the Mössbauer-absorption spectra are derived on the basis of the dispersion theory, for solid absorbers as well as for systems of interacting fine particles. The formulas give the spectra in a form of a superposition of a great many Lorentzian lines of the natural width. These formulas can be written in an approximate form, according to which the spectra are expressed as a superposition of several spectral components that are related with different categories of vibrational modes. From the exact and the approximate formulas, information about the detailed structure of the spectra is derived, including the intensities, linewidths, line shifts, and line shapes of the spectral components. In particular, for the systems of interacting fine particles, we demonstrate the existence of broad lines due to the particle-oscillation modes, observable with Mössbauer spectroscopy. The discussion is extended to multigrade-structured systems of interacting particles. Classical formulas are also derived and compared with the quantum-mechanical ones, leading to a criterion for the validity of the classical theory. Comparison with the experimental data shows that the present theory satisfactorily explains the experiments.

I. INTRODUCTION

Diffusive motions of various categories cause broad lines in Mössbauer spectra in addition to the usual unshifted narrow lines. Extensive studies have been done on this phenomenon both experimentally and theoretically.[1-11]

Similar broad lines appear in the Mössbauer spectra for systems consisting of semimicroscopic components of appropriate size (referred to as "fine particles" in this paper), which are bound to and can oscillate against each other; for example, a system of packed or sintered microcrystals. The existence of the broad lines [we shall call them "particle-oscillation lines (PO lines)"] has been shown theoretically[12,13] by the use of a simple classical theory of the Mössbauer effect developed by Shapiro,[14] but the result was only semiquantitative. Formation of a PO line means a reduction in recoilless fraction by an amount equal to its absorption area in addition to the reduction due to the formation of the usual phonon wing. This has been demonstrated by many experimental studies,[12,13,15-23] which have shown that the recoilless fraction is smaller for packed or sintered microcrystals than for the corresponding bulk specimens.

Recently, broad lines were clearly observed in ^{197}Au Mössbauer spectra of sintered copper microcrystals and interpreted as the PO lines.[24] This provided the first experimental evidence for the existence of the low-frequency vibrational modes in the sinters, which had been thought to be one of the principal origins of the anomalous Kapitza resistance between liquid helium and sintered metal heat exchangers in the millikelvin temperature range.[25,26]

The purpose of the present paper is to show quantum mechanically that the broad lines are caused by the oscillations of fine particles. For this purpose, formulas for the absorption cross section for a γ ray of an arbitrary energy will be derived on the basis of the dispersion theory, for solid absorbers as well as for systems of interacting fine particles. Investigation of these formulas demonstrates the existence of the PO line; moreover, it reveals many detailed features of the Mössbauer spectra, which is an extension of the theoretical studies of the spectral shape developed in the early days of the theory of Mössbauer effect.[27,28] Classical formulas for the absorption spectra are also derived, and the result is compared with the quantum-mechanical result. By doing so, the validity and limit of the classical theory are elucidated. In the present paper, the second-order Doppler shift is not taken into account. Oscillations are treated within the range of harmonic approximation. Moreover, we restrict ourselves to cubic symmetry in treating the crystals and particle systems for simplicity but without loss of generality.

The obtained formulas are compared with experimental data of ^{197}Au Mössbauer spectra of packed and sintered fine particles of gold and copper-gold alloy. It will be shown that the experimental spectra are satisfactorily accounted for by the present formulas with reasonable values of the parameters appearing in the formulas.

II. THEORY

A. Quantum-mechanical absorption cross section

According to the dispersion theory, the cross section of absorption of a γ ray of energy E by a single nucleus in a system of interacting atoms is given by

$$\sigma_a(E)=\frac{\sigma_0\Gamma_0^2}{4}\sum_{n,n_0} g_{n_0}\frac{|\langle n|\exp(i\mathbf{p}\cdot\mathbf{r}/\hbar)|n_0\rangle|^2}{(E_0-E+\varepsilon_n-\varepsilon_{n_0})^2+(\Gamma_0/2)^2}\ , \tag{1}$$

where $\mathbf{p}$ is the momentum of the γ ray, $\mathbf{r}$ the coordinate of the nucleus, and E_0 the energy difference between the final and the initial nuclear state. ε_n and ε_{n_0} are, respec-

tively, the energies of states $|n\rangle$ and $|n_0\rangle$ of the interacting system, Γ_0 is the natural width of the excited state of the nucleus, g_{n_0} is the statistical weight factor for the state $|n_0\rangle$, and σ_0 is the resonance absorption cross section.

By the use of the time-dependent correlation function method developed by van Hove,[29] it can be shown that for monatomic crystals of cubic symmetry Eq. (1) is written as[28]

$$\sigma_a(E)=\frac{\sigma_0\Gamma_0}{4\hbar}\int_{-\infty}^{\infty}\exp\left[-\frac{it}{\hbar}(E-E_0)-\frac{\Gamma_0}{2\hbar}|t|\right]\times\exp[-\tfrac{1}{2}\kappa^2\gamma_a(t)]dt\ . \tag{2}$$

In Eq. (2), $\hbar\boldsymbol{\kappa}=\mathbf{p}$ and $\gamma_a(t)$ represents a correlation between the displacements and is given by

$$\gamma_a(t)=2[\langle u_x(0)^2\rangle_{T_a}-\langle u_x(0)u_x(t)\rangle_{T_a}]\ , \tag{3}$$

where $\mathbf{u}(t)$ is the displacement of the atom from the equilibrium point at time t, the x axis is taken parallel to the direction of $\boldsymbol{\kappa}$, T_a is the temperature of the absorber, and $\langle\ \rangle_{T_a}$ stands for the thermal average at temperature T_a. Equation (3) is calculated to be

$$\gamma_a(t)=\frac{\hbar}{m_0}\sum_{m=1}^{3M}\frac{|a_m|^2}{\omega'_m}\left[\coth\left[\frac{\hbar\omega'_m}{2k_BT_a}\right](1-\cos\omega'_mt)-i\sin\omega'_mt\right]\ , \tag{4}$$

where k_B is the Boltzmann constant, m_0 the mass of an atom, M the number of atoms in the crystal, ω'_m the angular frequency of the mth mode, a_m's are the coefficients in expressing u_x as a linear combination of the normal-mode variables, and $|a_m|^2$ gives the phonon spectrum of the crystal and satisfies the relation $\sum_{m=1}^{3M}|a_m|^2=1$.

Inserting Eq. (4) into Eq. (2), we obtain (see Appendix)

$$\sigma_a(E)=\frac{\sigma_0\Gamma_0^2}{4}\left[\prod_{m=1}^{3M}\frac{2e^{-Y_m}}{Y_m}\right]\sum_{\{\mu_m\}}\sum_{\{\eta_m\}}\left[\prod_{m=1}^{3M}J_{\mu_m-\eta_m}(y_m)E_{\eta_m}(Y_m)\right]\frac{1}{\left[E-E_0-\hbar\sum_{m=1}^{3M}\mu_m\omega'_m\right]^2+(\Gamma_0/2)^2}\ , \tag{5}$$

where

$$y_m=\frac{|a_m|^2\hbar\kappa^2}{2m_0\omega'_m}\ , \tag{6}$$

$$Y_m=y_m\coth\left[\frac{\hbar\omega'_m}{2k_BT_a}\right]\ , \tag{7}$$

and

$$E_\eta(Y)=\sum_{\sigma=0}^{\infty}(|\eta|+2\sigma+1)I_{|\eta|+2\sigma+1}(Y)\ . \tag{8}$$

In Eqs. (5) and (8), $J_n(z)$ and $I_n(z)$ are a Bessel function and a modified Bessel function, respectively, $\sum_{\{\eta_m\}}$ denotes a summation over all sets of $3M$ integers $\{\eta_m\}$, in which each element can take on arbitrary values from $-\infty$ to ∞.

For a system of interacting fine particles (hereafter referred to as "particle aggregate"), Eq. (2) is still valid if the particle aggregate is isotropic or of cubic symmetry. The displacement of the nucleus is now due to both lattice phonon (ph) and particle oscillation (PO). If ph and PO are assumed to be independent of each other, $\gamma_a(t)$ can be expressed as a sum of two independent parts:

$$\gamma_a(t)=\gamma_a^{\rm ph}(t)+\gamma_a^{\rm PO}(t)\ . \tag{9}$$

In Eq. (9), $\gamma_a^{\rm ph}(t)$ is given by the right-hand side of Eq. (4), M now denoting the number of atoms in a particle. If rotational oscillations of the particles are neglected, and the aggregate is treated as a cubic Bravais lattice of the particles, $\gamma_a^{\rm PO}(t)$ is given by

$$\gamma_a^{\rm PO}(t)=\frac{\hbar}{M_0}\sum_{n=1}^{3N}\frac{|\alpha_n|^2}{\Omega'_n}\left[\coth\left[\frac{\hbar\Omega'_n}{2k_BT_a}\right](1-\cos\Omega'_nt)-i\sin\Omega'_nt\right]\ , \tag{10}$$

where M_0 is the mass of a particle, N the number of particles in the system, Ω'_n the angular frequency of nth mode, and $|\alpha_n|^2$'s give the frequency distribution of PO and satisfy the condition $\sum_{n=1}^{3N}|\alpha_n|^2=1$. Inserting Eqs. (4), (9), and (10) into Eq. (2) yields

$$\sigma_a(E)=\frac{\sigma_0\Gamma_0^2}{4}\left[\prod_{m=1}^{3M}\frac{2e^{-Y_m}}{Y_m}\right]\left[\prod_{n=1}^{3N}\frac{2e^{-\Upsilon_n}}{\Upsilon_n}\right]\times\sum_{\{\mu_m\}}\sum_{\{\eta_m\}}\sum_{\{\nu_n\}}\sum_{\{\zeta_n\}}\left[\prod_{m=1}^{3M}J_{\mu_m-\eta_m}(y_m)E_{\eta_m}(Y_m)\right]\left[\prod_{n=1}^{3N}J_{\nu_n-\zeta_n}(\upsilon_n)E_{\zeta_n}(\Upsilon_n)\right]\times\frac{1}{\left[E-E_0-\hbar\sum_{m=1}^{3M}\mu_m\omega'_m-\hbar\sum_{n=1}^{3N}\nu_n\Omega'_n\right]^2+(\Gamma_0/2)^2}\ , \tag{11}$$

where

$$v_n=\frac{|\alpha_n|^2\hbar\kappa^2}{2M_0\Omega_n'} \tag{12}$$

and

$$\Upsilon_n=v_n\coth\left[\frac{\hbar\Omega_n'}{2k_BT_a}\right] . \tag{13}$$

Investigation of Eqs. (5) and (11) reveals that the integrated intensity (absorption area) of the whole spectrum is equal to $\frac{1}{2}\pi\sigma_0\Gamma_0$ in both cases. From Eq. (5) we obtain (see the Appendix)

$$\int_{-\infty}^{\infty}\sigma_a(E)dE/\tfrac{1}{2}\pi\sigma_0\Gamma_0=\left[\prod_{m=1}^{3M}\frac{2e^{-Y_m}}{Y_m}\right]\sum_{\{\mu_m\}}\sum_{\{\eta_m\}}\left[\prod_{m=1}^{3M}J_{\mu_m-\eta_m}(y_m)E_{\eta_m}(Y_m)\right]=1 . \tag{14}$$

Similarly, integrating Eq. (11) yields

$$\begin{aligned}\int_{-\infty}^{\infty}\sigma_a(E)dE/\tfrac{1}{2}\pi\sigma_o\Gamma_0=&\left[\prod_{m=1}^{3M}\frac{2e^{-Y_m}}{Y_m}\right]\left[\sum_{\{\mu_m\}}\sum_{\{\eta_m\}}\left[\prod_{m=1}^{3M}J_{\mu_m-\eta_m}(y_m)E_{\eta_m}(Y_m)\right]\right]\\&\times\left[\prod_{n=1}^{3N}\frac{2e^{-\Upsilon_n}}{\Upsilon_n}\right]\left[\sum_{\{\nu_n\}}\sum_{\{\xi_n\}}\left[\prod_{n=1}^{3N}J_{\nu_n-\xi_n}(v_n)E_{\xi_n}(\Upsilon_n)\right]\right]=1\times1=1 .\end{aligned} \tag{15}$$

These are natural results and can be obtained directly from Eq. (1).

In Eq. (5), the component corresponding to $\{\mu_m\}=\{0\}$, where $\{0\}$ is the set for which all elements are equal to zero, represents the recoilless Mössbauer line (M line). Therefore, the recoilless fraction (RF) for a crystal is written

$$\begin{aligned}(\mathrm{RF})_{\mathrm{cryst}}=&\int_{-\infty}^{\infty}\sigma_a^M(E)dE/\tfrac{1}{2}\pi\sigma_0\Gamma_0\\=&\left[\prod_{m=1}^{3M}\frac{2e^{-Y_m}}{Y_m}\right]\sum_{\{\eta_m\}}\left[\prod_{m=1}^{3M}J_{-\eta_m}(y_m)E_{\eta_m}(Y_m)\right] .\end{aligned} \tag{16}$$

We shall call the last expression of Eq. (16) f_a:

$$f_a=\left[\prod_{m=1}^{3M}\frac{2e^{-Y_m}}{Y_m}\right]\sum_{\{\eta_m\}}\left[\prod_{m=1}^{3M}J_{-\eta_m}(y_m)E_{\eta_m}(Y_m)\right] , \tag{17}$$

which can approximately be written

$$\begin{aligned}f_a\simeq&\exp\left[-\sum_{m=1}^{3M}Y_m\right]=\exp\left[-\frac{1}{2}\kappa^2\gamma_a(\infty)\right]\\=&\exp(-\kappa^2\langle u_x^2\rangle_{T_a}) ,\end{aligned} \tag{18}$$

since the right-hand side of Eq. (17) is rewritten

$$\left[\prod_{m=1}^{3M}\frac{2e^{-Y_m}}{Y_m}\right]\prod_{m=1}^{3M}\left[\sum_{\eta=-\infty}^{\infty}J_\eta(y_m)E_\eta(Y_m)\right]$$

and

$$\sum_{\eta=-\infty}^{\infty}J_\eta(y_m)E_\eta(Y_m)\simeq Y_m/2 .$$

In obtaining the last two equalities in Eq. (18) we have used the relation

$$\sum_{m=1}^{3M}Y_m=\frac{1}{2}\kappa^2\gamma_a(\infty)=\kappa^2\langle u_x^2\rangle_{T_a} ,$$

which follows from Eqs. (3), (4), (6), and (7). If we write $e'=Y/3M$, where Y is a typical value of

$$\frac{\hbar\kappa^2}{2m_0\omega_m'}\coth\left[\frac{\hbar\omega_m'}{2k_BT_a}\right] ,$$

the relative error of Eq. (18) is less than e'. For a particle aggregate, the M line corresponds to the combination of sets $\{\mu_m\}=\{0\}$ and $\{\nu_n\}=\{0\}$ in Eq. (11), and we have

$$\begin{aligned}(\mathrm{RF})_{\mathrm{aggr}}=&\left[\prod_{m=1}^{3M}\frac{2e^{-Y_m}}{Y_m}\right]\left[\sum_{\{\eta_m\}}\left[\prod_{m=1}^{3M}J_{-\eta_m}(y_m)E_{\eta_m}(Y_m)\right]\right]\\&\times\left[\prod_{n=1}^{3N}\frac{2e^{-\Upsilon_n}}{\Upsilon_n}\right]\left[\sum_{\{\xi_n\}}\left[\prod_{n=1}^{3N}J_{-\xi_n}(v_n)E_{\xi_n}(\Upsilon_n)\right]\right]=f_aF_a ,\end{aligned} \tag{19}$$

where

$$F_a=\left[\prod_{n=1}^{3N}\frac{2e^{-\Upsilon_n}}{\Upsilon_n}\right]\left[\sum_{\{\zeta_n\}}\left[\prod_{n=1}^{3N}J_{-\zeta_n}(\upsilon_n)E_{\zeta_n}(\Upsilon_n)\right]\right], \tag{20}$$

which is approximated

$$F_a\simeq\exp\left[-\sum_{n=1}^{3N}\Upsilon_n\right]=\exp\left[-\frac{1}{2}\kappa^2\gamma_a^{\mathrm{PO}}(\infty)\right]$$
$$=\exp[-\kappa^2\langle(u_x^{\mathrm{PO}})^2\rangle_{T_a}]\,. \tag{21}$$

Hence Eq. (19) can be rewritten in an approximate form

$$(\mathrm{RF})_{\mathrm{aggr}}\simeq\exp\left[-\sum_{m=1}^{3M}Y_m\right]\exp\left[-\sum_{n=1}^{3N}\Upsilon_n\right]$$
$$=\exp[-\kappa^2\langle(u_x^{\mathrm{ph}})^2\rangle_{T_a}]\exp[-\kappa^2\langle(u_x^{\mathrm{PO}})^2\rangle_{T_a}]$$
$$=\exp(-\kappa^2\langle u_x^2\rangle_{T_a})\,. \tag{22}$$

The relative error of Eq. (22) is less than $e'+\varepsilon'$, where $\varepsilon'=\Upsilon/3N$, Υ being a typical value of

$$\frac{\hbar\kappa^2}{2M_0\Omega_n'}\coth\left[\frac{\hbar\Omega_n'}{2k_BT_a}\right].$$

Since generally both e' and ε' are very small quantities, Eqs. (18) and (22) hold to a very good approximation.

The probability of γ absorption without a change in ph state regardless of PO state equals

$$\left[\prod_{m=1}^{3M}\frac{2e^{-Y_m}}{Y_m}\right]\left[\sum_{\{\eta_m\}}\left[\prod_{m=1}^{3M}J_{-\eta_m}(y_m)E_{\eta_m}(Y_m)\right]\right]\left[\prod_{n=1}^{3N}\frac{2e^{-\Upsilon_n}}{\Upsilon_n}\right]\left[\sum_{\{\nu_n\}}\sum_{\{\zeta_n\}}\left[\prod_{n=1}^{3N}J_{\nu_n-\zeta_n}(\upsilon_n)E_{\zeta_n}(\Upsilon_n)\right]\right]=f_a\times1=f_a\,. \tag{23}$$

Similarly, the probability of γ absorption without a change in PO state regardless of ph state is found to be F_a. Thus, we obtain for all components of the spectrum the integrated intensities normalized to that for the whole spectrum: For a crystal the intensities are equal to f_a and $1-f_a$ for the M line and the phonon wing (ph band), respectively, while for a particle aggregate they are equal to f_aF_a, $f_a(1-F_a)$, $(1-f_a)F_a$, and $(1-f_a)(1-F_a)$ for the M line, PO line, ph band, and the component involving both ph and PO excitations (ph·PO band), respectively. Here the PO line and ph band refer to the components involving only PO and ph excitations, respectively.

For a crystal, the average energy transferred to the lattice is calculated using Eq. (5) (see the Appendix):

$$\langle E-E_0\rangle=\int_{-\infty}^{\infty}(E-E_0)\sigma_a(E)dE/\tfrac{1}{2}\pi\sigma_0\Gamma_0=R\,, \tag{24}$$

where

$$R=\hbar^2\kappa^2/2m_0=E_0^2/2m_0c^2$$

is the recoil energy of a free nucleus. Similarly, for a particle aggregate, we obtain by the use of Eq. (11) (see the Appendix)

$$\langle E-E_0\rangle=R+P\,. \tag{25}$$

for the average energy transferred to ph and/or PO, where

$$P=\hbar^2\kappa^2/2M_0=E_0^2/2M_0c^2$$

is the recoil energy of a free particle.

The sum rule (24) has been proven by Lipkin[30] in a general way, on the assumption that the interatomic forces in the crystal depend only upon the positions of the atoms and not upon their velocities. The extended sum rule (25) also can generally be proven by assuming that the interparticle forces in the aggregate depend only upon the positions of the particles and not upon their velocities. If the coordinate of the nucleus is given by $\mathbf{R}+\boldsymbol{\rho}$, where $\mathbf{R}$ is the coordinate of the center of mass of the particle and $\boldsymbol{\rho}$ the coordinate of the nucleus with respect to the center of mass of the particle, we then obtain

$$(\{H,\exp[i\boldsymbol{\kappa}\cdot(\mathbf{R}+\boldsymbol{\rho})]\},\exp[-i\boldsymbol{\kappa}\cdot(\mathbf{R}+\boldsymbol{\rho})])$$
$$=-\frac{(\hbar\kappa)^2}{m_0}-\frac{(\hbar\kappa)^2}{M_0}\,, \tag{26}$$

where H is the Hamiltonian for the entire system. Writing Eq. (26) as a matrix equation and taking the diagonal element for the state $|n_0\rangle$, we obtain

$$\sum_n[E(n)-E(n_0)]P(n,n_0)=\frac{(\hbar\kappa)^2}{2m_0}+\frac{(\hbar\kappa)^2}{2M_0}=R+P\,, \tag{27}$$

where $E(n)$ and $E(n_0)$ are the energies of the system for the states $|n\rangle$ and $|n_0\rangle$, respectively, and $P(n,n_0)$ is the probability of transition from $|n_0\rangle$ to $|n\rangle$.

Since the M lines do not contribute to the sum rules, the average shifts of other components should be larger than those required by the sum rules. For a crystal, the average shift of the ph band equals (see the Appendix)

$$\langle E-E_0\rangle^{\mathrm{ph}}=\int_{-\infty}^{\infty}(E-E_0)\sigma_a^{\mathrm{ph}}(E)dE/\tfrac{1}{2}\pi\sigma_0\Gamma_0(1-f_a)$$
$$=R/(1-f_a)\,. \tag{28}$$

Similarly, for a particle aggregate, the average shifts of the components are found to be $P/(1-F_a)$, $R/(1-f_a)$, and $R/(1-f_a)+P/(1-F_a)$ for the PO line, ph band, and ph·PO band, respectively. These results combined with the calculated integrated intensities of the components exactly conform to the sum rules.

B. Classical absorption cross section

According to the classical theory,[14] when a γ ray of frequency $\omega_0=E_0/\hbar$ is incident on a crystal, the frequency observed by the absorbing nucleus is modulated by the motion of the nucleus itself in the lattice. The phase of the γ wave seen by the nucleus is

$$\Psi(t)=\omega_0(t)-\kappa_0 u_x(t) ,$$

where $\kappa_0=\omega_0/c$, c being the velocity of light, and $u_x(t)$ is the displacement of the nucleus in the direction of the γ ray. If the motion of the nucleus is given by a superposition of harmonic oscillations:

$$u_x(t)=\sum_{m=1}^{3M} u_m \sin(\omega'_m t+\theta_m) , \tag{29}$$

then the vector potential of the γ wave at the position of the nucleus is written

$$\begin{aligned} A(t)&= A_0 e^{-|t|/\tau_0} e^{i\Psi(t)} \\ &= A_0 e^{-|t|/\tau_0} \sum_{\{\mu_m\}} \left[\prod_{m=1}^{3M} J_{\mu_m}(\kappa_0 u_m)\right] \\ &\quad \times \exp\left\{ i \left[\left[\omega_0+\sum_{m=1}^{3M} \mu_m \omega'_m \right] t+\sum_{m=1}^{3M} \mu_m \theta_m \right] \right\} . \end{aligned} \tag{30}$$

In Eq. (30), the factor $e^{-|t|/\tau_0}$ has been introduced in order to make the γ wave of finite duration. The frequency spectrum is obtained by taking the Fourier transform of Eq. (30):

$$F(\omega)=\left[\frac{2}{\pi}\right]^{1/2} A_0 \sum_{\{\mu_m\}} \left[\prod_{m=1}^{3M} J_{\mu_m}(\kappa_0 u_m)\right] \exp\left[i \sum_{m=1}^{3M} \mu_m \theta_m \right] \frac{1/\tau_0}{\left[\omega-\omega_0-\sum_{m=1}^{3M} \mu_m \omega'_m\right]^2+(1/\tau_0)^2} . \tag{31}$$

Equation (30) describes an electromagnetic wave which is a superposition of a great many partial waves. Each partial wave corresponds to a set $\{\mu_m\}$ and has a frequency $\omega_0+\sum_{m=1}^{3M}\mu_m\omega'_m$, and its intensity is

$$|A_0|^2 e^{-2|t|/\tau_0} \prod_{m=1}^{3M} J^2_{\mu_m}(\kappa_0 u_m) .$$

The amount of energy $\hbar\sum_{m=1}^{3M}\mu_m\omega'_m$ in excess of $\hbar\omega_0$ should be Doppler compensated for the partial wave to be resonantly absorbed. The sum of intensities over all partial waves equals $|A_0|^2 e^{-2|t|/\tau_0}$, since

$$\sum_{\{\mu_m\}} \left[\prod_{m=1}^{3M} J^2_{\mu_m}(\kappa_0 u_m)\right] = \prod_{m=1}^{3M} \left[\sum_{\mu=-\infty}^{\infty} J^2_{\mu}(\kappa_0 u_m)\right] = 1 .$$

The M line corresponds to the set $\{0\}$, and its intensity equals

$$|A_0|^2 e^{-2|t|/\tau_0} \prod_{m=1}^{3M} J^2_0(\kappa_0 u_m) .$$

Thus the probability of the recoilless absorption (RF) for a crystal is

$$(\mathrm{RF})_{\mathrm{cryst}}=\prod_{m=1}^{3M} J^2_0(\kappa_0 u_m) \simeq \exp(-\kappa_0^2 \langle u_x^2 \rangle_{T_a}) . \tag{32}$$

The second equality in Eq. (32) is valid because of the extreme smallness of u_m's. The last expression in the equation is very close to f_a, the quantum-mechanical RF given by Eq. (17). The total absorption probability of the partial waves that make up the ph band is, therefore, $1-f_a$.

For a particle aggregate, we assume that

$$u_x(t)=u_x^{\mathrm{ph}}(t)+u_x^{\mathrm{PO}}(t) ,$$

where $u_x^{\mathrm{ph}}(t)$ is given by Eq. (29) with u_m replaced by u_m^{ph}, while $u_x^{\mathrm{PO}}(t)$ is given by

$$u_x^{\mathrm{PO}}(t)=\sum_{n=1}^{3N} u_n^{\mathrm{PO}} \sin(\Omega'_n t+\phi_n) .$$

Then we have

$$\begin{aligned} A(t)&= A_0 e^{-|t|/\tau_0} \sum_{\{\mu_m\}} \sum_{\{\nu_n\}} \left[\prod_{m=1}^{3M} J_{\mu_m}(\kappa_0 u_m^{\mathrm{ph}})\right] \left[\prod_{n=1}^{3N} J_{\nu_n}(\kappa_0 u_n^{\mathrm{PO}})\right] \\ &\quad \times \exp\left\{ i \left[\left[\omega_0+\sum_{m=1}^{3M} \mu_m \omega'_m+\sum_{n=1}^{3N} \nu_n \Omega'_n \right] t+\sum_{m=1}^{3M} \mu_m \theta_m+\sum_{n=1}^{3N} \nu_n \phi_n \right] \right\} , \end{aligned} \tag{33}$$

$$F(\omega)=\left[\frac{2}{\pi}\right]^{1/2} A_0 \sum_{\{\mu_m\}} \sum_{\{\nu_n\}} \left[\prod_{m=1}^{3M} J_{\mu_m}(\kappa_0 u_m^{\mathrm{ph}})\right] \left[\prod_{n=1}^{3N} J_{\nu_n}(\kappa_0 u_n^{\mathrm{PO}})\right] \exp\left[i \left[\sum_{m=1}^{3M} \mu_m \theta_m+\sum_{n=1}^{3N} \nu_n \phi_n \right] \right]$$

$$\times \frac{1/\tau_0}{\left[\omega-\omega_0-\sum_{m=1}^{3M} \mu_m \omega'_m-\sum_{n=1}^{3N} \nu_n \Omega'_n\right]^2+(1/\tau_0)^2} . \tag{34}$$

In Eq. (33), each partial wave corresponds to a combination of two sets $\{\mu_m\}$ and $\{\nu_n\}$, and has a frequency

$$\omega_0+\sum_{m=1}^{3M}\mu_m\omega'_m+\sum_{n=1}^{3N}\nu_n\Omega'_n$$

and an intensity

$$|A_0|^2e^{-2|t|/\tau_0}\left[\prod_{m=1}^{3M}J^2_{\mu_m}(\kappa_0 u_m^{\rm ph})\right]\left[\prod_{n=1}^{3N}J^2_{\nu_n}(\kappa_0 u_n^{\rm PO})\right].$$

The total intensity of all partial waves equals $|A_0|^2e^{-2|t|/\tau_0}$ also in this case. The M line corresponds to the sets $\{\mu_m\}=\{0\}$ and $\{\nu_n\}=\{0\}$, and its intensity is

$$|A_0|^2e^{-2|t|/\tau_0}\left[\prod_{m=1}^{3M}J_0^2(\kappa_0 u_m^{\rm ph})\right]\left[\prod_{n=1}^{3N}J_0^2(\kappa_0 u_n^{\rm PO})\right].$$

The absorption probabilities for the M line, PO line, ph bands, and ph·PO bands are to a very good approximation equal to f_aF_a, $f_a(1-F_a)$, $(1-f_a)F_a$, and $(1-f_a)(1-F_a)$, respectively, where f_a and F_a are the quantum-mechanical RF's.

Comparison of the classical frequency spectra (31) and (34) with the quantum-mechanical counterparts, Eqs. (5) and (11), shows that both theories coincide in number and position of the partial lines, but not in their intensities except for the M line. For Eq. (31), two partial lines, respectively corresponding to $\{\mu_m\}$ and $\{\mu'_m\}$, for which $\mu_m=-\mu'_m$ for all m's have equal intensities because of the relation $J^2_\mu(z)=J^2_{-\mu}(z)$, and their positions are at equal distances from $\omega=\omega_0$ on opposite sides. Therefore, the ph band is unshifted and symmetrical in shape. It is verified in similar way that, for Eq. (34), all the components including the PO line, ph band, and ph·PO band are unshifted and symmetrical. Thus the classical theory utterly fails in explaining the shifts of the components required by the sum rules.

C. Approximate formulas for the quantum-mechanical absorption cross section

If continuous functions are used for representing ph and PO energy-level distributions, then $\gamma_a(t)$ [Eq. (3)] becomes[28]

$$\gamma_a^{\rm ph}(t)=\frac{\hbar^2}{m_0}\int_0^\infty\left[\coth\left[\frac{z}{2k_BT_a}\right]\left[1-\cos\frac{zt}{\hbar}\right]-i\sin\frac{zt}{\hbar}\right]\frac{\phi_a(z)}{z}dz \tag{35}$$

for ph, and

$$\gamma_a^{\rm PO}(t)=\frac{\hbar^2}{M_0}\int_0^\infty\left[\coth\left[\frac{z}{2k_BT_a}\right]\left[1-\cos\frac{zt}{\hbar}\right]-i\sin\frac{zt}{\hbar}\right]\frac{\Phi_a(z)}{z}dz \tag{36}$$

for PO. The distribution functions $\phi_a(z)$ and $\Phi_a(z)$ are normalized in such a way that

$$\int_0^\infty\phi_a(z)dz=\int_0^\infty\Phi_a(z)dz=1\ ,$$

moreover, $\phi_a(z)$ and $\Phi_a(z)$ are zero beyond $z_{\rm max}^{\rm ph}$ and $z_{\rm max}^{\rm PO}$, respectively.

$\gamma_a^{\rm ph}(t)$ can approximately be written[28]

$$\frac{1}{2}\kappa^2\gamma_a^{\rm ph}(t)=-iR\frac{t}{\hbar}+\delta^2\frac{t^2}{4\hbar^2}\quad\text{for } |t|\ll\tau\ , \tag{37a}$$

$$=\tfrac{1}{2}\kappa^2\gamma_a^{\rm ph}(\infty)\quad\text{for } |t|\gg\tau\ , \tag{37b}$$

where $\tau=\hbar/z_{\rm max}^{\rm ph}$ and

$$\delta^2=2R\int_0^\infty z\coth\left[\frac{z}{2k_BT_a}\right]\phi_a(z)dz\ . \tag{38}$$

Adopting the approximations (37a) and (37b) in the ranges $|t|<\tau$ and $|t|>\tau$, respectively, $\sigma_a(E)$ for a crystal can be written, using Eq. (2),

$$\sigma_a(E)=\frac{\sigma_0\Gamma_0}{4\hbar}\exp\left[-\frac{1}{2}\kappa^2\gamma_a^{\rm ph}(\infty)\right]\left[\int_{-\infty}^{-\tau}+\int_\tau^\infty\right]\exp\left[-\frac{it}{\hbar}(E-E_0)-\frac{\Gamma_0}{2\hbar}|t|\right]dt$$
$$+\frac{\sigma_0\Gamma_0}{4\hbar}\int_{-\tau}^{\tau}\exp\left[-\frac{it}{\hbar}(E-E_0)-\frac{\Gamma_0}{2\hbar}|t|+iR\frac{t}{\hbar}-\frac{\delta^2}{4\hbar^2}t^2\right]dt\ . \tag{39}$$

Setting

$$F_1(t)=\exp\left[-\frac{it}{\hbar}(E-E_0)-\frac{\Gamma_0}{2\hbar}|t|\right],$$

$$F_2(t)=\exp\left[-\frac{it}{\hbar}(E-E_0)-\frac{\Gamma_0}{2\hbar}|t|+iR\frac{t}{\hbar}-\frac{\delta^2}{4\hbar^2}t^2\right],$$

the integrals in Eq. (39) can be written

$$\left[\int_{-\infty}^{-\tau}+\int_\tau^\infty\right]F_1(t)dt=\left[\int_{-\infty}^{\infty}-\int_{-\tau}^{\tau}\right]F_1(t)dt$$
$$=(1-A)\int_{-\infty}^{\infty}F_1(t)dt\ , \tag{40a}$$

$$\int_{-\tau}^{\tau}F_2(t)dt=\left[\int_{-\infty}^{\infty}-\left[\int_{-\infty}^{-\tau}+\int_\tau^\infty\right]\right]F_2(t)dt$$
$$=(1-B)\int_{-\infty}^{\infty}F_2(t)dt\ . \tag{40b}$$

It is found that A is negligibly small if

$$\Gamma_0\tau/2\hbar=\Gamma_0/2z_{\max}^{\mathrm{ph}}\ll 1 .$$

It is shown that $\ln B$ is of the order of $\delta^2\tau^2/\hbar^2$, while

$$\tfrac{1}{2}\kappa^2\gamma_a^{\mathrm{ph}}(\infty)=\kappa^2\langle(u_x^{\mathrm{ph}})^2\rangle_{T_a}$$

is also of the order of $\delta^2\tau^2/\hbar^2$. Therefore we assume that $B=f_a(\simeq\exp[-\frac{1}{2}\kappa^2\gamma_a^{\mathrm{ph}}(\infty)])$, which satisfies the requirement that the total integrated intensity be equal to $\frac{1}{2}\pi\sigma_0\Gamma_0$, as can be seen in the following. Thus we obtain for a crystal

$$\sigma_a(E)=\frac{\sigma_0\Gamma_0^2}{4}f_a\frac{1}{(E-E_0)^2+(\Gamma_0/2)^2}+\frac{\pi^{1/2}\sigma_0\Gamma_0}{2\delta}(1-f_a)\exp\left[-\frac{(E-E_0-R)^2}{\delta^2}\right] . \tag{41}$$

In calculating the integral $\int_{-\infty}^{\infty}F_2(t)dt$, the second Parseval theorem in the Fourier transform theory has been used. The first and the second term in Eq. (41) describe a Lorentzian line of width [full width at half maximum (FWHM)] Γ_0 and a Gaussian line of width (FWHM) $2(\ln 2)^{1/2}\delta$, and represent the M line and the ph band, respectively.

For PO, $\gamma_a^{\mathrm{PO}}(t)$ can be approximated

$$\frac{1}{2}\kappa^2\gamma_a^{\mathrm{PO}}(t)=-iP\frac{t}{\hbar}+\Delta^2\frac{t^2}{4\hbar^2}\quad\text{for } |t|\ll T , \tag{42a}$$

$$=\tfrac{1}{2}\kappa^2\gamma_a^{\mathrm{PO}}(\infty)\quad\text{for } |t|\gg T , \tag{42b}$$

where $T=\hbar/z_{\max}^{\mathrm{PO}}$, and

$$\Delta^2=2P\int_0^{\infty}z\coth\left[\frac{z}{2k_BT_a}\right]\Phi_a(z)dz . \tag{43}$$

Then, dividing the range of integration $(-\infty,\infty)$ in Eq. (2) into subranges $(-\infty,-T)$, $(-T,-\tau)$, $(-\tau,\tau)$, (τ,T), and (T,∞), and adopting the approximations (37a), (37b), (42a), and (42b) in the ranges $|t|<\tau$, $|t|>\tau$, $|t|<T$, and $|t|>T$, respectively, we obtain for a particle aggregate, with the help of Eq. (9),

$$\sigma_a(E)=\frac{\sigma_0\Gamma_0^2}{4}f_aF_a\frac{1}{(E-E_0)^2+(\Gamma_0/2)^2}+\frac{\pi^{1/2}\sigma_0\Gamma_0}{2\Delta}f_a(1-F_a)\exp\left[-\frac{(E-E_0-P)^2}{\Delta^2}\right]+\frac{\pi^{1/2}\sigma_0\Gamma_0}{2(\delta^2+\Delta^2)^{1/2}}(1-f_a)\exp\left[-\frac{(E-E_0-R-P)^2}{\delta^2+\Delta^2}\right] , \tag{44}$$

where the factors f_aF_a, $f_a(1-F_a)$, and $(1-f_a)$ have been determined in the same way as the factors in Eq. (41) were determined. The first and the second term in Eq. (44) represent the M line and the PO line, respectively. The third term is interpreted as representing the sum of the ph band and ph·PO band, which are practically inseparable. According to the equation, the widths of these components are Γ_0, $2(\ln 2)^{1/2}\Delta$, and

$$2[\ln 2(\delta^2+\Delta^2)]^{1/2} ,$$

respectively.

Integrating Eqs. (41) and (44), we find that the total integrated intensity is equal to $\frac{1}{2}\pi\sigma_0\Gamma_0$ for both equations. We also find that the integrated intensities of various components calculated on these approximate formulas are equal to those due to the exact formulas (5) and (11). However, there is some discrepancy in the shifts of the components between the approximate and the exact formulas, although they are in order-of-magnitude agreement. Therefore, the sum rules are not rigorously satisfied by the approximate formulas.

III. EXPERIMENTAL RESULTS

Figure 1 shows ^{197}Au absorption spectra obtained at 16 K in gold fine particles of 50 nm average diameter packed

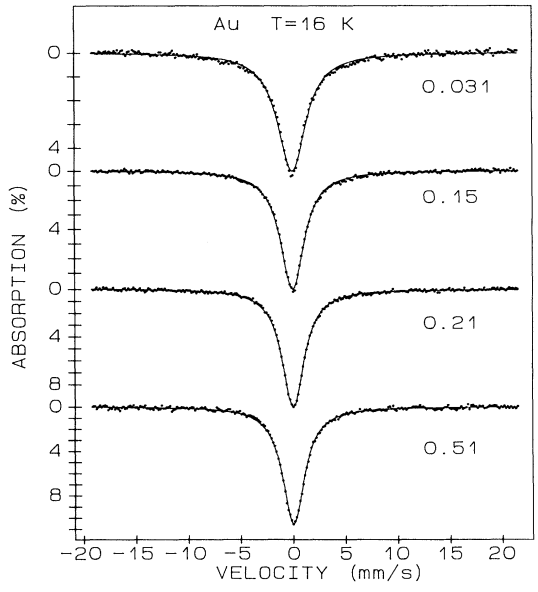

FIG. 1. Mössbauer spectra at 16 K of Au fine particles of 50 nm average diameter packed to various packing fractions. The figures indicate the packing fractions. The solid lines represent the least-squares-fitted Lorentzians.

to various packing fractions.[31] In Fig. 2(a) are shown the spectra at different temperatures of sintered copper fine particles of 150 nm average particle diameter and 26.7% packing fraction, which are doped with 3.60 at. % gold.[24] Figure 2(b) shows the spectra of the Cu-Au alloy powder sample, in which the particles have the same composition and size as the particles of Fig. 2(a) and are loosely packed without sintering to a packing fraction approximately equal to 2%.[24] In these figures, the solid lines represent the least-squares-fitted Lorentzian lines. It is found that there is a systematic discrepancy between the experimental data and the fitted curves: At the minimum point of the absorption line the experimental data project beyond the theoretical curve, the data retreat behind the curve on both sides of the line, and again exceed the curve on the foot of the line. This discrepancy becomes larger with decreasing packing fraction (Fig. 1) or increasing temperature [Figs. 2(a) and 2(b)].

The discrepancy between the experimental data and the fitted curves suggests that a broad component is overlapping the Lorentzian line. According to the theoretical model described in Sec. II, this additional component is ascribed to the PO line, which has a Gaussian line shape according to the approximate formula (44). Fitting the spectra with a Lorentzian line and a Gaussian one, better fits are obtained, as is shown in Fig. 3 for the Au powder sample and Figs. 4(a) and 4(b) for the Cu-Au sinter and Cu-Au powder samples, respectively. The experimental spectra are to be compared with the formulas for the self-absorption cross section $\sigma(s)$, where $s=(v/c)E_0$ is the energy Doppler shift caused by moving the emitter with velocity v relative to the absorber. It is found that $\sigma(s)$ has the same shape as $\sigma_a(E)$ except that the width of the M line is approximately doubled (increased by the source linewidth), the width of ph band is increased by a factor of about $2^{1/2}$, and the shift of ph band is increased by R.[24] The two-component fitting is unsuccessful for the spectra of the Au powder samples of 21% and 51% packing fractions. This is because the depths of the Gaussian components are so small for these samples that an accurate analysis is impossible on account of the statistical scatter in the spectra.

For the Cu-Au samples, for which the measurements have been done with varying temperature, the absolute values of the recoilless fractions f_a and F_a can be deduced from the temperature dependence of the absorption area of the M line, provided the shapes of the distribution functions $\phi_a(z)$ and $\Phi_a(z)$ are known.[24] Using the Debye model for ph in the particles and the fracton model for PO in the samples, according to which $\Phi_a(z)$ is approximately a flat function, we obtain $\Theta=206$ K, $z_1/k_B=3.99$ mK for the sinter and 2.00 mK for the powder, and $z_2/k_B=198$ mK for the sinter and 183 mK for the powder, where Θ is the Debye temperature for the Au impurity atoms in the alloy, and z_1 and z_2 are the

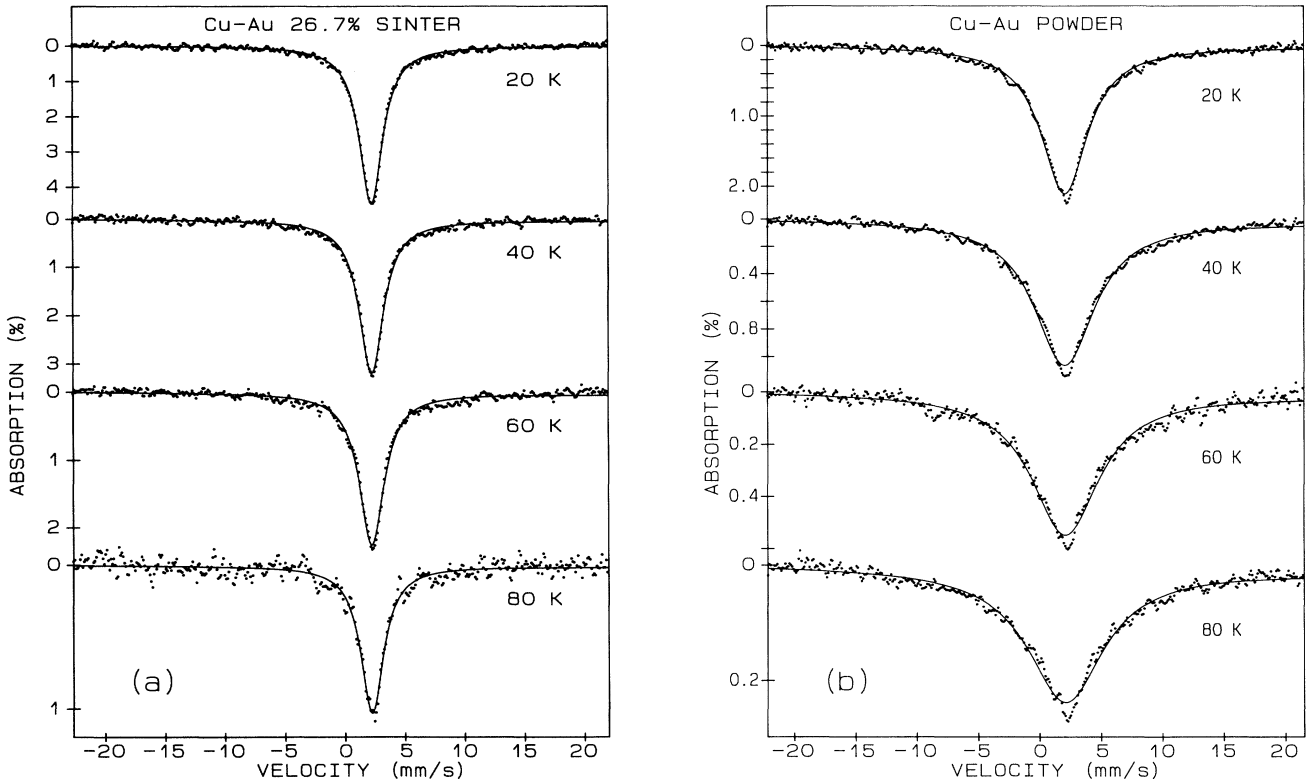

FIG. 2. Mössbauer spectra at different temperatures of Cu—3.60 at. % Au fine particles of 150 nm average diameter in (a) a sintered sample of 26.7% packing fraction and (b) a powder sample of ~2% packing fraction. The solid lines represent the least-squares-fitted Lorentzians.

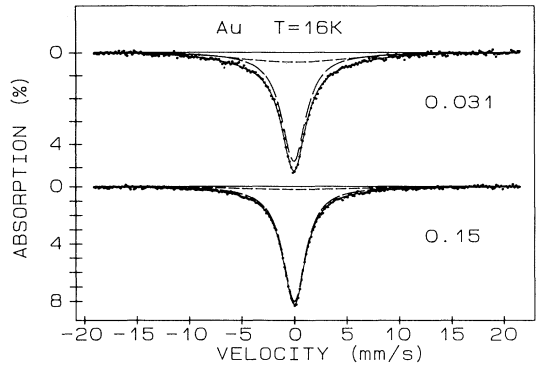

FIG. 3. Two-component (Lorentzian-plus-Gaussian) fitting of the Mössbauer spectra of Au powder samples. Solid line: fitted absorption curve; long-dashed line: Lorentzian component; short-dashed line: Gaussian component.

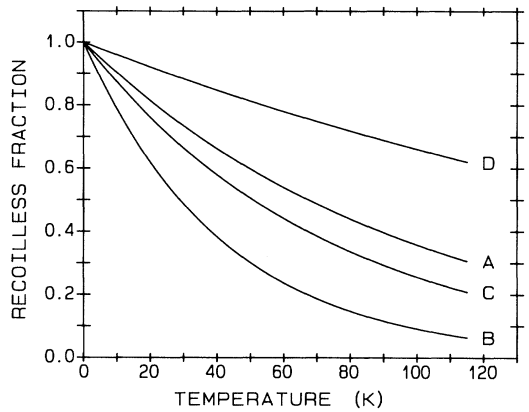

FIG. 5. Temperature dependence of the calculated recoilless fractions F_a and $\mathcal{F}_a$ for Cu-Au samples. *A*: F_a for sinter; *B*: F_a for powder sample obtained without considering cluster oscillation; *C*: F_a for powder sample obtained considering cluster oscillation; *D*: $\mathcal{F}_a$ for powder sample.

lower and upper limit, respectively, of the energy range of the flat function $\Phi_a(z)$.[24] The saturation effect has been taken into account in the calculation.[24] The Debye temperature Θ was determined from the data on a Cu-Au alloy foil with the same composition as the fine particles, which had been prepared and measured for purposes of comparison. The resulting values of F_a are shown as functions of temperature in Fig. 5. Using the deduced values of f_a and F_a, we obtain the effective absorber thickness t_a, from which the saturation-effect-corrected values of Γ_{obs}, the observed linewidth (FWHM) of the *M* line, can be determined. The corrected linewidths are plotted in Fig. 6, in which the data for the Cu-Au foil are also plotted.

IV. DISCUSSION AND CONCLUSION

Exact formulas for the absorption cross-section spectra have been derived for crystals and for particle aggregates

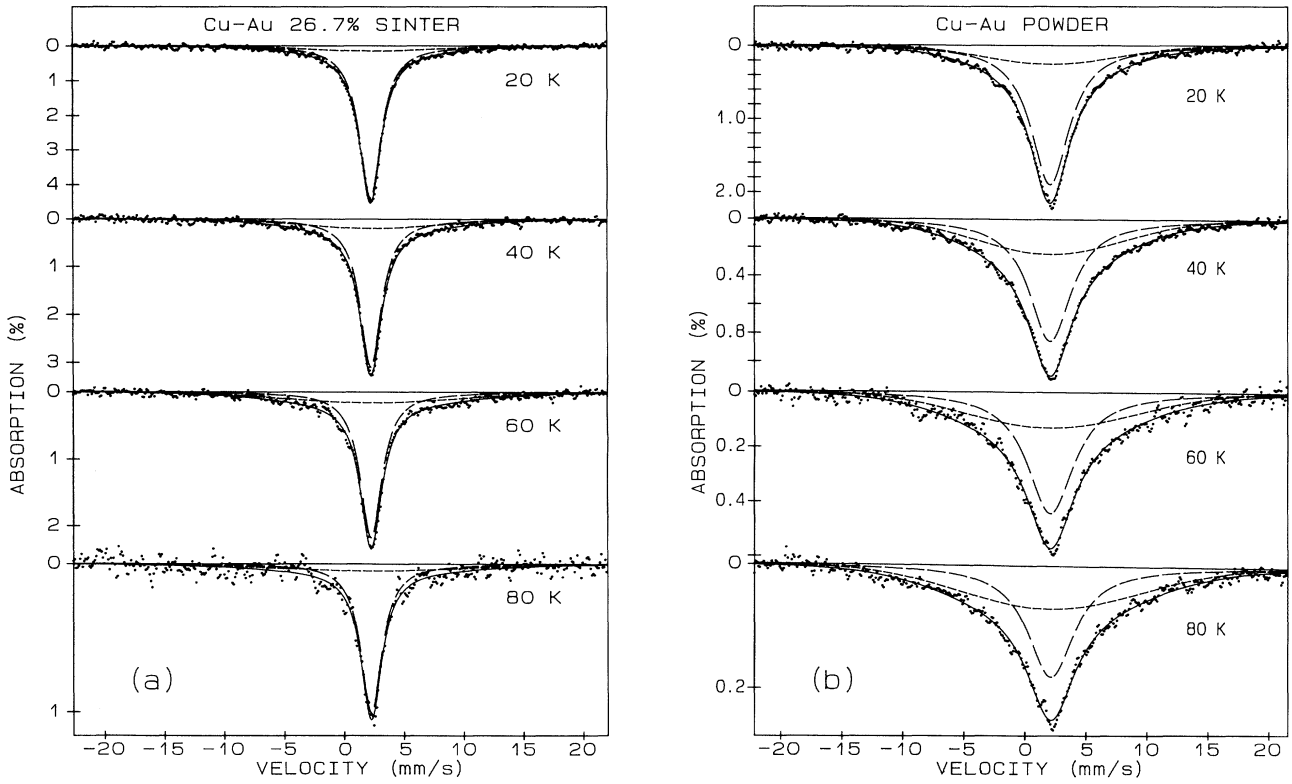

FIG. 4. Two-component (Lorentzian-plus-Gaussian) fitting of the Mössbauer spectra of (a) Cu-Au sintered sample and (b) Cu-Au powder sample. Solid line: fitted absorption curve; long-dashed line: Lorentzian component; short-dashed line: Gaussian component.

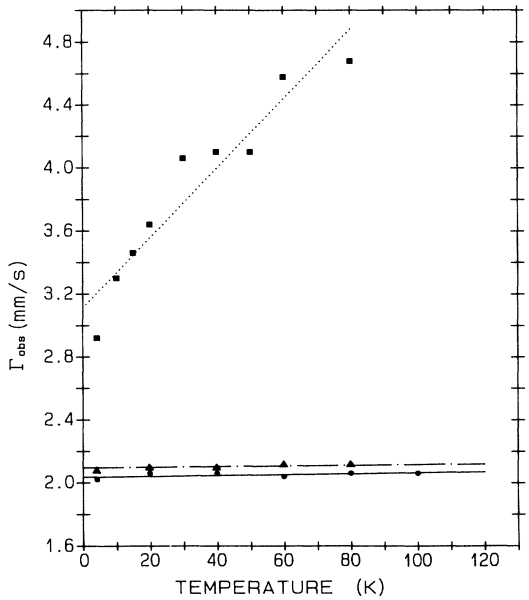

FIG. 6. Plot of the saturation-effect-corrected linewidth Γ_{obs} of the Lorentzians determined by Lorentzian-plus-Gaussian fit as a function of temperature for Cu-Au samples. Closed circle: foil; closed triangle: sinter; closed square: powder. The straight lines are the least-squares-fits to the data.

on the basis of the dispersion theory (Sec. II A). The result shows that the spectrum consists of a great many lines of width Γ_0, which are shifted by the energies transferred to ph and/or PO. These lines are divided into a number of spectrum components (M line, PO line, ph band, etc.) according to their physical origins. Integrated intensities of these components were obtained from the formulas; for a crystal the normalized intensities are f_a and $1-f_a$ for the M line and ph band, respectively, while for a particle aggregate they are equal to f_aF_a, $f_a(1-F_a)$, $(1-f_a)F_a$, and $(1-f_a)(1-F_a)$ for the M line, PO line, ph band, and ph·PO band, respectively. Here f_a and F_a are the RF's due to ph and PO, respectively, and are given by Eqs. (17) and (20). These quantities can be written

$$f_a=\exp[-\kappa^2\langle(u_x^{\rm ph})^2\rangle_{T_a}]$$

and

$$F_a=\exp[-\kappa^2\langle(u_x^{\rm PO})^2\rangle_{T_a}]$$

to a very good approximation. The shifts of the components were also calculated; for a crystal the shift of the ph band equals $R/(1-f_a)$, while for a particle aggregate the shifts are $P/(1-F_a)$, $R/(1-f_a)$, and $R/(1-f_a)+P/(1-F_a)$ for the PO line, ph band, and ph·PO band, respectively, where R and P are the recoil energies of a free nucleus and a free particle, respectively. These results exactly conform to the sum rules, which require that the average energy transfer equals R for crystals and $R+P$ for particle aggregates.

It will be difficult to deduce the shape of a component as a whole from the exact formulas and determine its width and peak value, except for the M line. On the other hand, in the approximate formulas derived in Sec. II C, each term on the right-hand side of the equations corresponds to a component of the spectrum, and its shape, width, peak value, and shift are explicitly given. This makes the approximate formulas very useful. Although the sum rules are not rigorously satisfied by these formulas, they give correct values for the integrated intensities of the components, and their shifts are of reasonable magnitudes (in order-of-magnitude correct).

Because of the largeness of width and shift [Eqs. (28), (38), and (43)], the ph band and ph·PO band always disappear into the background in usual Mössbauer spectra. On the other hand, the PO line can be observed in the spectra under some circumstances because its shift is always small and its width can have an appropriate value to be observed in the Mössbauer spectrum. Since Ω_n''s are usually very low, the width is determined primarily by M_0, the mass of a particle, hence the "appropriate size of the particle" is essential for the observability of the PO line.

To our surprise, for all components the integrated intensities deduced from the classical theory agree with the quantum-mechanical results to a very good approximation. On the other hand, the classical theory cannot explain the shifts of the components. This is natural because the classical theory merely calculates the frequency spectrum of the electromagnetic waves observed by the oscillating nucleus, assuming that the amount of absorbed energy is proportional to the intensity of the wave, and does not take into account the momentum transfer accompanying the energy absorption. Even if due account is taken of the momentum transfer, the quantum-mechanical values R or P will not result from a purely classical treatment.

Experimental results on packed or sintered fine particles of metallic Au or Cu-Au alloy are compared with the present theory (Sec. III). In the spectra the broad lines due to PO excitations are clearly observed. The deduced values of the parameters Θ, z_1, and z_2 are of reasonable magnitude. The values of z_1 and z_2 are in fairly good agreement with the results obtained from the mechanical and ultrasonic measurements.[24]

In the present study, it has been quantum mechanically proven that there exists a broad line (PO line) superimposed on the M line in the spectra of systems of two-grade structure consisting of atoms and fine particles. The broad lines are very similar in shape to those caused by diffusive motions of the absorbing nuclei, but the present lines are due to the hierarchical structure of the oscillations in the absorber. It is noted that the broad lines appear even in the harmonic range of the oscillations. If small particles exist in clusters and the interclustery forces are much weaker than the intraclustery forces, then we have a three-grade structured system consisting of atoms, particles, and clusters. There will now appear in the spectrum a new component due to the oscillations of the clusters, and the cluster-oscillation line (CO line) will have a Gaussian line shape and be much narrower than the PO line. In this case, the integrated intensities of the components in the spectrum are equal to

$f_a F_a \mathcal{F}_a$(M line), $f_a F_a(1-\mathcal{F}_a)$ (CO line), $f_a(1-F_a)\mathcal{F}_a$ (PO line), $f_a(1-F_a)(1-\mathcal{F}_a)$ (PO·CO line), $(1-f_a)F_a\mathcal{F}_a$ (ph band), etc., where $\mathcal{F}_a$ is the RF due to CO. The sum rule becomes

$$\langle E-E_0\rangle = R+P+Q \ ,$$

where Q is the recoil energy of a free cluster. The shifts of the components are equal to $Q/(1-\mathcal{F}_a)$ (CO line), $P/(1-F_a)$ (PO line), $P/(1-F_a)+Q/(1-\mathcal{F}_a)$ (PO·CO line), $R/(1-f_a)$ (ph band), etc. Since Q is much smaller than P, the PO line and the PO·CO line are inseparable, hence there are practically three components in the spectrum in addition to the M line, i.e., the CO line (PO+PO·CO) line, and the band made up of the components involving ph excitations, among which only the former two can be observed in the Mössbauer spectrum. It is evident that we can proceed in this way to many-grade structured systems, having a new line each time we have a new grade, and the new line being always narrower than the preceding one. However, the linewidth cannot be smaller than Γ_0, and if the width of the new line becomes very close to Γ_0, the new line cannot be distinguished from the M line, hence the new grade can have no effect on the spectrum. In the series of hierarchical systems consisting of atoms, microcrystals, clusters, clusters of clusters, etc., the three-grade system will perhaps be the one with the largest number of grade which can be studied by the Mössbauer spectroscopy.

From Fig. 6 we see that the observed linewidths of M line ($\Gamma_{\rm obs}$) for the sinter and the foil nearly agree with each other and remain constant as the temperature varies, whereas $\Gamma_{\rm obs}$ for the powder is much larger than those for the former two and rapidly increases with increasing temperature. The experimental data projecting beyond the peaks of the fitted curves in Fig. 4(b) are indicative of the presence of narrow lines of natural width. This suggests that in powder samples the fine particles exist in clusters and there is in the spectra a CO line overlapping the M line. If a Lorentzian and two Gaussian lines are fitted to the spectra, fits are further improved as is shown in Fig. 7. In the fitting, the linewidth of the Lorentzian line has been fixed at the value of $\Gamma_{\rm obs}$ of the foil. From the temperature dependence of absorption area of the new M line, the values of z_1, z_2, $\varkappa_1$, and $\varkappa_2$ are deduced, where z_1 and z_2 are the lower and upper limit of the energy range of the new distribution function $\Phi_a(z)$ for PO while $\varkappa_1$ and $\varkappa_2$ are those for CO. The result is that z_1/k_B, z_2/k_B, $\varkappa_1/k_B$, and $\varkappa_2/k_B$ are equal to 2.4, 234, 2.8, and 75 mK, respectively. These values are reasonable. The theoretical curves $F_a(T)$ and $\mathcal{F}_a(T)$ calculated using these values of z's and $\varkappa$'s are shown in Fig. 5. In the calculation, the average cluster size has been assumed to be nine times the average particle size, since the linewidth of the (PO+PO·CO) line is approximately three times that of the CO line at all temperatures investigated (Fig. 7).

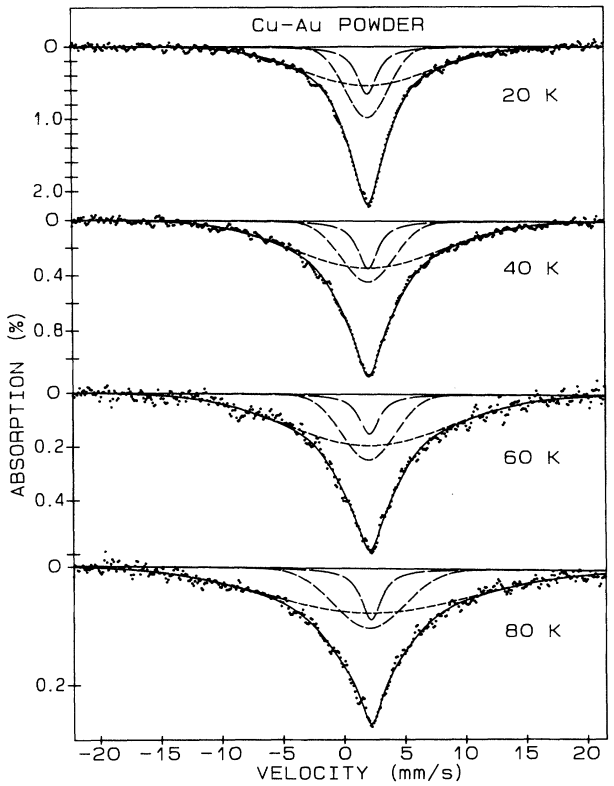

FIG. 7. Three-component (Lorentzian-plus-two-Gaussians) fitting of the Mössbauer spectra of Cu-Au powder sample. Solid line: fitted absorption curve; long-dashed line: Lorentzian component; medium-dashed line: Gaussian component due to CO; short-dashed line: Gaussian component due to PO and PO·CO.

ACKNOWLEDGMENT

The author thanks Dr. I. Tamura of Toyama Medical and Pharmaceutical University for his help in the data analysis.

APPENDIX: DERIVATION OF THE EQUATIONS

1. Equation (5)

$$\sigma_a(E)=\frac{\sigma_0\Gamma_0}{4\hbar}\int_{-\infty}^{\infty}\exp\left[-\frac{it}{\hbar}(E-E_0)-\frac{\Gamma_0}{2\hbar}|t|\right]\prod_{m=1}^{3M}\left[e^{-Y_m}e^{Y_m\cos\omega'_m t}e^{iy_m\sin\omega'_m t}\right]dt$$

$$=\frac{\sigma_0\Gamma_0}{4\hbar}\int_{-\infty}^{\infty}\exp\left[-i\omega t-\frac{\Gamma_0}{2\hbar}|t|\right]\prod_{m=1}^{3M}\left[\frac{2e^{-Y_m}}{Y_m}\left[\sum_{n=0}^{\infty}(n+1)I_{n+1}(Y_m)\sum_{r=0}^{n}\cos(2r-n)\omega'_m t\right]\right.$$

$$\times\left[\sum_{p=-\infty}^{\infty} J_p(y_m)e^{ip\omega'_m t}\right]\Bigg]dt$$

$$=\frac{\sigma_0\Gamma_0}{4\hbar}\int_{-\infty}^{\infty}\exp\left[-i\omega t-\frac{\Gamma_0}{2\hbar}|t|\right]\left[\prod_{m=1}^{3M}\frac{2e^{-Y_m}}{Y_m}\right]\sum_{\{\eta_m\}}\left[\prod_{m=1}^{3M}E_{\eta_m}(Y_m)\cos\eta_m\omega'_m t\right]$$

$$\times\sum_{\{p_m\}}\left\{\left[\prod_{m=1}^{3M}J_{p_m}(y_m)\right]\exp\left[i\left[\sum_{m=1}^{3M}p_m\omega'_m\right]t\right]\right\}dt$$

$$=\frac{\sigma_0\Gamma_0}{2^{3M+1}\hbar}\int_{-\infty}^{\infty}e^{-(\Gamma_0/2\hbar)|t|}\left[\prod_{m=1}^{3M}\frac{2e^{-Y_m}}{Y_m}\right]\sum_{\{\eta_m\}}\left\{\left[\prod_{m=1}^{3M}E_{\eta_m}(Y_m)\right]\right.$$

$$\left.\times\left[\sum_{s=0}^{(3M-1)/2}{}^{(3M}C_s)\sum^{(3M-s)}\cos\left[\sum^{(3M-s)}\eta_m\omega'_m-\sum^{(s)}\eta_m\omega'_m\right]t\right]\right\}$$

$$\times\sum_{\{p_m\}}\left\{\left[\prod_{m=1}^{3M}J_{p_m}(y_m)\right]\exp\left[i\left[\sum_{m-1}^{3M}p_m\omega'_m-\omega\right]t\right]\right\}dt \tag{A1}$$

$$=\frac{\sigma_0\Gamma_0^2}{4}\left[\prod_{m=1}^{3M}\frac{2e^{-Y_m}}{Y_m}\right]\sum_{\{\mu_m\}}\sum_{\{\eta_m\}}\left[\prod_{m=1}^{3M}J_{\mu_m-\eta_m}(y_m)E_{\eta_m}(Y_m)\right]$$

$$\times\frac{1}{\left[E-E_0-\hbar\sum_{m=1}^{3M}\mu_m\omega'_m\right]^2+(\Gamma_0/2)^2}\,, \tag{5}$$

where $\hbar\omega=E-E_0$. In expression (A1), $\sum^{(3M-s)}$ denotes a sum of $(3M-s)$ members selected from the set $\eta_m\omega'_m$ $(m=1,2,\ldots,3M)$, while $\sum^{(s)}$ is the sum of the rest members, and $\sum^{(3M}{}^{C_s)}$ indicates that the sum is taken over all such combinations. In (A1), it is assumed that M is an odd integer: If M is even, the expression is somewhat different, but the final result (5) is the same.

2. Equation (14)

$$\int_{-\infty}^{\infty}\sigma_a(E)dE/\tfrac{1}{2}\pi\sigma_0\Gamma_0=\left[\prod_{m=1}^{3M}\frac{2e^{-Y_m}}{Y_m}\right]\sum_{\{\mu_m\}}\sum_{\{\eta_m\}}\left[\prod_{m=1}^{3M}J_{\mu_m-\eta_m}(y_m)E_{\eta_m}(Y_m)\right]$$

$$=\left[\prod_{m=1}^{3M}\frac{2e^{-Y_m}}{Y_m}\right]\left[\prod_{m=1}^{3M}\left[\sum_{\xi=-\infty}^{\infty}J_\xi(y_m)\right]\right]\left[\prod_{m=1}^{3M}\left[\sum_{\eta=-\infty}^{\infty}E_\eta(Y_m)\right]\right] \tag{A2}$$

$$=\left[\prod_{m=1}^{3M}\frac{2e^{-Y_m}}{Y_m}\right]\times1\times\left[\prod_{m=1}^{3M}\frac{Y_m}{2}e^{Y_m}\right]=1\,. \tag{14}$$

In obtaining (A2), we used new variables $\xi_m=\mu_m-\eta_m$.

3. Equations (24) and (25)

$$\langle E-E_0\rangle=\int_{-\infty}^{\infty}(E-E_0)\sigma_a(E)dE/\tfrac{1}{2}\pi\sigma_0\Gamma_0$$

$$=\left[\prod_{m=1}^{3M}\frac{2e^{-Y_m}}{Y_m}\right]\sum_{\{\mu_m\}}\sum_{\{\eta_m\}}\left[\hbar\sum_{m=1}^{3M}\mu_m\omega'_m\right]\left[\prod_{m=1}^{3M}J_{\mu_m-\eta_m}(y_m)E_{\eta_m}(Y_m)\right]$$

$$=\hbar\left[\prod_{m=1}^{3M}\frac{2e^{-Y_m}}{Y_m}\right]\left\{\left[\sum_{\{\xi_m\}}\left[\sum_{m=1}^{3M}\xi_m\omega'_m\right]\prod_{m=1}^{3M}J_{\xi_m}(y_m)\right]\left[\sum_{\{\eta_m\}}\prod_{m=1}^{3M}E_{\eta_m}(Y_m)\right]\right.$$

$$\left.+\left[\sum_{\{\xi_m\}}\prod_{m=1}^{3M}J_{\xi_m}(y_m)\right]\left[\sum_{\{\eta_m\}}\left[\sum_{m=1}^{3M}\eta_m\omega'_m\right]\prod_{m=1}^{3M}E_{\eta_m}(Y_m)\right]\right\}$$

$$=\hbar\left[\prod_{m=1}^{3M}\frac{2e^{-Y_m}}{Y_m}\right]\left\{\left[\sum_{m=1}^{3M}y_m\omega'_m\right]\left[\prod_{m=1}^{3M}\left[\frac{1}{2}Y_m e^{Y_m}\right]\right]+1\times0\right\}$$

$$=\hbar\sum_{m=1}^{3M}y_m\omega'_m=R\,, \tag{24}$$

$$\langle E-E_0\rangle=\left[\prod_{m=1}^{3M}\frac{2e^{-Y_m}}{Y_m}\right]\left[\prod_{n=1}^{3N}\frac{2e^{-\Upsilon_n}}{\Upsilon_n}\right]\sum_{\{\mu_m\}}\sum_{\{\eta_m\}}\sum_{\{\nu_n\}}\sum_{\{\xi_n\}}\left[\hbar\sum_{m=1}^{3M}\mu_m\omega'_m+\hbar\sum_{n=1}^{3N}\nu_n\Omega'_n\right]\left[\prod_{m=1}^{3M}J_{\mu_m-\eta_m}(y_m)E_{\eta_m}(Y_m)\right]\times\left[\prod_{n=1}^{3N}J_{\nu_n-\zeta_n}(\upsilon_n)E_{\zeta_n}(\Upsilon_n)\right]$$

$$=R+P\ . \tag{25}$$

In the above calculations, we have used the relations:

$$y_m=|a_m|^2(R/\hbar\omega'_m)\ \text{ and }\ \upsilon_n=|\alpha_n|^2(P/\hbar\Omega'_n)\ .$$

4. Equation (28)

$$\langle E-E_0\rangle^{\rm ph}=\int_{-\infty}^{\infty}(E-E_0)\sigma_a^{\rm ph}(E)dE/\tfrac{1}{2}\pi\sigma_0\Gamma_0(1-f_a)$$

$$=\left[\prod_{m=1}^{3M}\frac{2e^{-Y_m}}{Y_m}\right]\sum_{\{\mu_m\}}^{0}\sum_{\{\eta_m\}}\left[\hbar\sum_{m=1}^{3M}\mu_m\omega'_m\right]\left[\prod_{m=1}^{3M}J_{\mu_m-\eta_m}(y_m)E_{\eta_m}(Y_m)\right]\Big/(1-f_a)$$

$$=\left[\prod_{m=1}^{3M}\frac{2e^{-Y_m}}{Y_m}\right]\sum_{\{\mu_m\}}\sum_{\{\eta_m\}}\left[\hbar\sum_{m=1}^{3M}\mu_m\omega'_m\right]\left[\prod_{m=1}^{3M}J_{\mu_m-\eta_m}(y_m)E_{\eta_m}(Y_m)\right]\Big/(1-f_a)$$

$$=R/(1-f_a)\ , \tag{28}$$

where $\sum_{\{\mu_m\}}^{0}$ denotes a summation over all sets $\{\mu_m\}$ except $\{0\}$.

[1]D. C. Champeney and F. W. D. Woodhams, J. Phys. B **1**, 620 (1968).

[2]H. Fraunfelder, G. A. Petsko, and D. Tsernoglou, Nature (London) **280**, 558 (1979).

[3]F. Parak, E. W. Knapp, and D. Kucheida, J. Mol. Biol. **161**, 177 (1982).

[4]E. W. Knapp, S. F. Fischer, and F. Parak, J. Chem. Phys. **78**, 4701 (1983).

[5]I. Nowik, E. R. Bauminger, S. G. Cohen, and S. Ofer, Phys. Rev. A **31**, 2291 (1985).

[6]G. Vogl, W. Mansel, and P. H. Dederichs, Phys. Rev. Lett. **36**, 1497 (1976).

[7]W. Petry, G. Vogl, and W. Mansel, Phys. Rev. Lett. **45**, 1862 (1980).

[8]W. Petry and G. Vogl, Z. Phys. B **45**, 207 (1982).

[9]W. Petry, G. Vogl, and W. Mansel, Z. Phys. B **46**, 319 (1982).

[10]R. Wordel, F. J. Litterst, and F. E. Wagner, J. Phys. F **15**, 2525 (1985).

[11]G. von Eynatten, T. Ritter, H. E. Bömmel, and K. Dransfeld, Z. Phys. B **65**, 341 (1987).

[12]M. Hayashi, I. Tamura, Y. Fukano, and S. Kanemaki, Phys. Lett. **77A**, 332 (1980).

[13]M. Hayashi, I. Tamura, Y. Fukano, and S. Kanemaki, Surf. Sci. **106**, 453 (1981).

[14]F. L. Shapiro, Usp. Fiz. Nauk **72**, 685 (1961) [Sov. Phys. Usp. **3**, 881 (1961)].

[15]I. P. Suzdalev, M. Ya. Gen, V. I. Gol'danskii, and E. F. Makarov, Zh. Eksp. Teor. Fiz. **51**, 118 (1966) [Sov. Phys. JETP **24**, 79 (1967)].

[16]S. Roth and E. M. Hörl, Phys. Lett. **25A**, 299 (1967).

[17]J. S. van Wieringen, Phys. Lett. **26A**, 370 (1968).

[18]S. Akselrod and M. Pasternak, Phys. Rev. B **11**, 1040 (1975).

[19]M. P. A. Viegers and J. M. Trooster, Phys. Rev. B **15**, 72 (1977).

[20]G. von Eynatten and H. E. Bömmel, Appl. Phys. **14**, 415 (1977).

[21]K. Haneda and A. H. Morrish, J. Phys. Suppl. C **2**, 91 (1979).

[22]P. Bussière, Rev. Phys. Appl. **15**, 1143 (1980).

[23]M. Hayashi, I. Tamura, Y. Fukano, S. Kanemaki, and Y. Fujio, J. Phys. C **13**, 681 (1980).

[24]M. Hayashi, E. Gerkema, A. M. van der Kraan, and I. Tamura, Phys. Rev. B **42**, 9771 (1990).

[25]N. Nishiguchi and T. Nakayama, Solid State Commun. **45**, 877 (1983).

[26]A. R. Rutherford, J. P. Harrison, and M. J. Stott, J. Low Temp. Phys. **55**, 157 (1984).

[27]W. M. Visscher, Ann. Phys. **9**, 194 (1960).

[28]K. S. Singwi and A. Sjölander, Phys. Rev. **120**, 1093 (1960).

[29]L. van Hove, Phys. Rev. **95**, 249 (1954).

[30]H. J. Lipkin, Ann. Phys. **9**, 332 (1960).

[31]M. Hayashi, I. Tamura, and H. Sakai, Jpn. J. Appl. Phys. **25**, L905 (1986).